Microglial subpopulations with distinct transcriptome signatures vary across brain regions in the resting mouse brain

Mishima, Rei
Taniguchi, Masayuki
Matsushita, Kazutoshi
Tian, Bowen
Furuyashiki, Tomoyuki

(Citation)
Journal of Pharmacological Sciences,151(3):142-147

(Issue Date)
2023-03

(Resource Type)
journal article

(Version)
Version of Record

(URL)
https://hdl.handle.net/20.500.14094/0100481905

Journal of Pharmacological Sciences 151 (2023) 142–147

Contents lists available at ScienceDirect

Journal of Pharmacological Sciences

journal homepage: www.elsevier.com/locate/jphs

Short communication

Microglial subpopulations with distinct transcriptome signatures vary across brain regions in the resting mouse brain

Rei Mishima, Masayuki Taniguchi, Kazutoshi Matsushita, Bowen Tian, Tomoyuki Furuyashiki*

Division of Pharmacology, Kobe University Graduate School of Medicine, 7-5-1 Kusunoki-cho, Chuo-ku, Kobe, 650-0017, Japan

ARTICLE INFO

Article history:
Received 7 December 2022
Received in revised form
23 December 2022
Accepted 27 December 2022
Available online 29 December 2022

Keywords:
Microglia
Heterogeneity
scRNA-seq

ABSTRACT

Microglia are crucial for tissue homeostasis and its disturbance. However, microglial heterogeneity and its relationship with microglial activation in physiological conditions remain elusive. Using single-cell RNA sequencing, we identified microglial subpopulations with distinct transcriptome signatures in the resting brain. The distribution of two major, continuous subpopulations varied across brain regions, especially between cerebral cortices and the hypothalamus. Lipopolysaccharide and chronic social defeat stress, both of which involve the innate immune receptor TLR4, upregulate the marker genes of selective microglial subpopulations. These findings suggest that microglial subpopulations contribute to the heterogeneity of microglial transcriptome and responsiveness within and across brain regions.

Microglia are resident immune cells in the brain, playing crucial roles for brain tissue homeostasis and damage.[1] In the resting and healthy brain, microglia continuously survey the brain parenchyma and contribute to neural circuit development and plasticity. In neurodegenerative and psychiatric conditions and aging, microglia change their properties, affecting neural functions via the secretion of proinflammatory mediators and phagocytic activity.[2,3] Single-cell RNA sequencing (scRNA-seq) revealed the heterogeneity of microglial transcriptome in neurodegenerative conditions, and identified a pathological microglial subtype named the disease-associated microglia (DAM).[4] scRNA-seq analysis also identified minor subsets of microglia expressing interferon-response genes and the chemokines CCL3/4, respectively, which increase with aging.[5] However, the heterogeneity of the major remaining subset of microglia has been suggested as microglial transcriptome in bulk RNA-seq analysis varies across brain regions. Furthermore, environmental stimuli such as chronic social defeat stress (CSDS) activate microglia without apparent neuronal loss, contributing to behavioral abnormalities, via the innate immune receptors Toll-like receptor 2 and 4 (TLR2/4).[6] However, the microglial heterogeneity in the resting brain and its relationship with stress-induced microglial activation remain to be examined at the single-cell resolution.

In this study, we investigated the single-cell heterogeneity of microglial transcriptome within and among brain regions in the resting brain and its relationship with microglial activation by the TLR4 ligand lipopolysaccharide (LPS) and CSDS. All animal experiments were approved by the Institutional Animal Care and Use Committee (P-200201-R6) and carried out according to the Kobe University Animal Experimentation Regulations. To this aim, we analyzed enhanced green fluorescent protein (EGFP)-expressing immune cells, including microglia, in multiple brain regions of a male CX3CR1-EGFP mouse (B6.129P2(Cg)-Cx3cr1tm1Litt/J, Jackson Laboratory) at 9 weeks old using scRNA-seq with Chromium system (10x Genomics) (Fig. 1A). The tissues of the prefrontal cortex (PFC), orbitofrontal cortex (OFC), primary sensorimotor cortex (M1S1), nucleus accumbens (NAc), hypothalamus (HYP), amygdala (AMY), and hippocampus (HIP) were mechanically dissociated without enzymatic reaction, as previously described.[7] The samples were kept on ice or at 4 °C, otherwise stated. We also analyzed murine microglia-like N9 cells (a kind gift from Dr. Makoto Tsuda) and human embryonic kidney (HEK) 293-like cells (AAV-293 cells, Agilent) cultured in Dulbecco's Modified Eagle's Medium (D-MEM) containing 5% and 10% fetal bovine serum (Thermo Fisher Scientific), respectively, and dispersed with *l*-trypsin at 37 °C for 1 min as controls (Fig. 1A). The samples were labelled with distinct barcodes (3' CellPlex, 10x Genomics) for multiplexing at room temperature for 5 min. Single-cell suspensions combined from multiple brain regions were subjected to cell sorting with FACSAria-III (Beckton Dickinson) to isolate EGFP-expressing cells. scRNA-seq analysis

* Corresponding author.
E-mail address: tfuruya@med.kobe-u.ac.jp (T. Furuyashiki).
Peer review under responsibility of Japanese Pharmacological Society.

https://doi.org/10.1016/j.jphs.2022.12.010

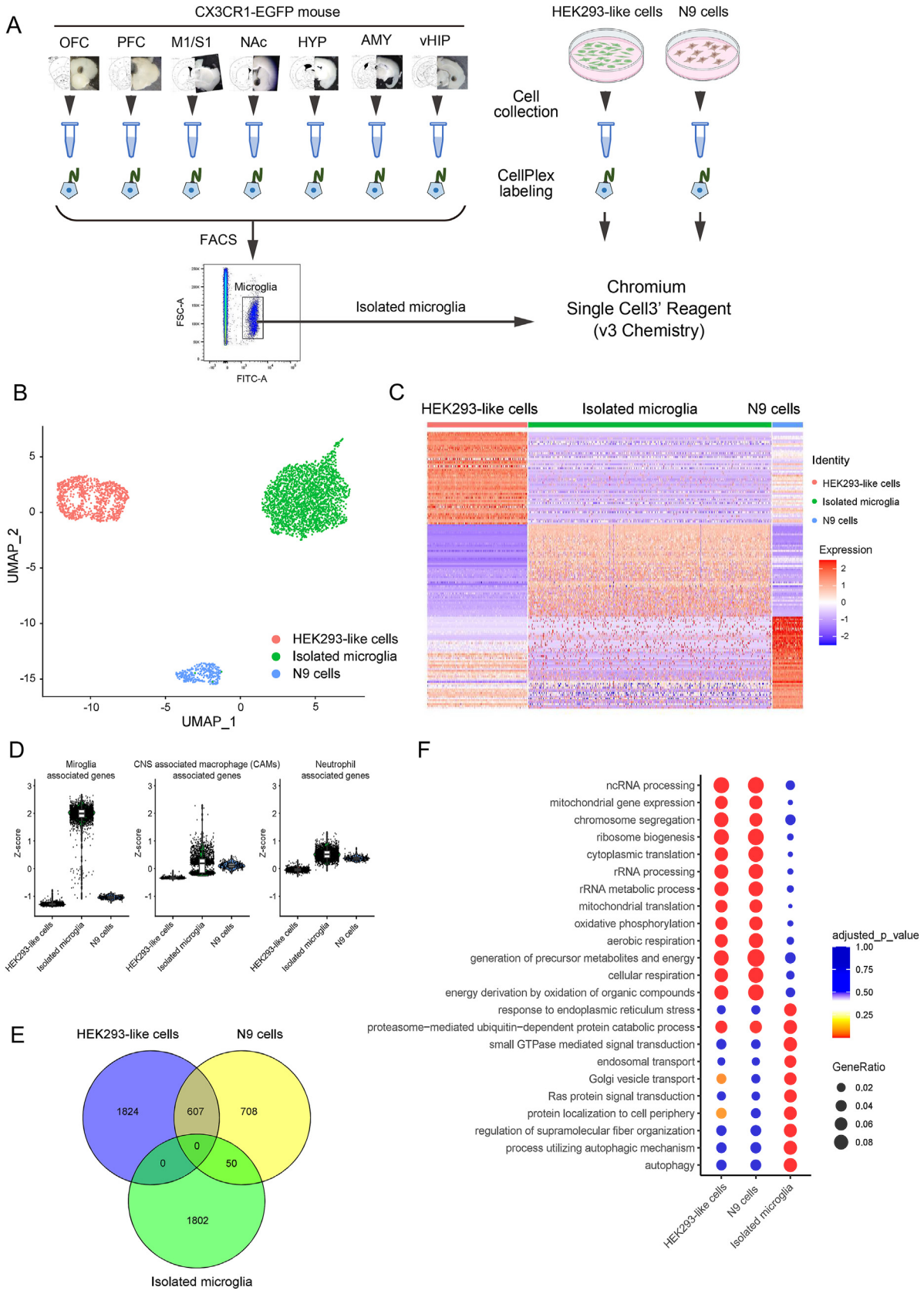

Fig. 1. Single-cell RNA-seq identifies transcriptome signatures of microglia in the resting brain.
(A) Experimental design. (B) UMAP plot showing the clusters of isolated microglia (2437 cells) from a male CX3CR1-EGFP mouse at 9 weeks old, N9 cells (302 cells), and HEK293-like cells (1004 cells). (C) Heatmap of marker genes of the three cell types. (D) Violin boxplots showing single-cell distribution of Z-scores averaged for the signature gene expressions of microglia, CNS-associated macrophage, and neutrophil for the three cell types identified with scRNA-seq shown in (A). (E) Venn diagrams of the marker genes. (F) Bubble chart showing GO terms enriched in the marker genes with the proportion of expressed genes (bubble size) and the adjusted P value of the enrichment (color).

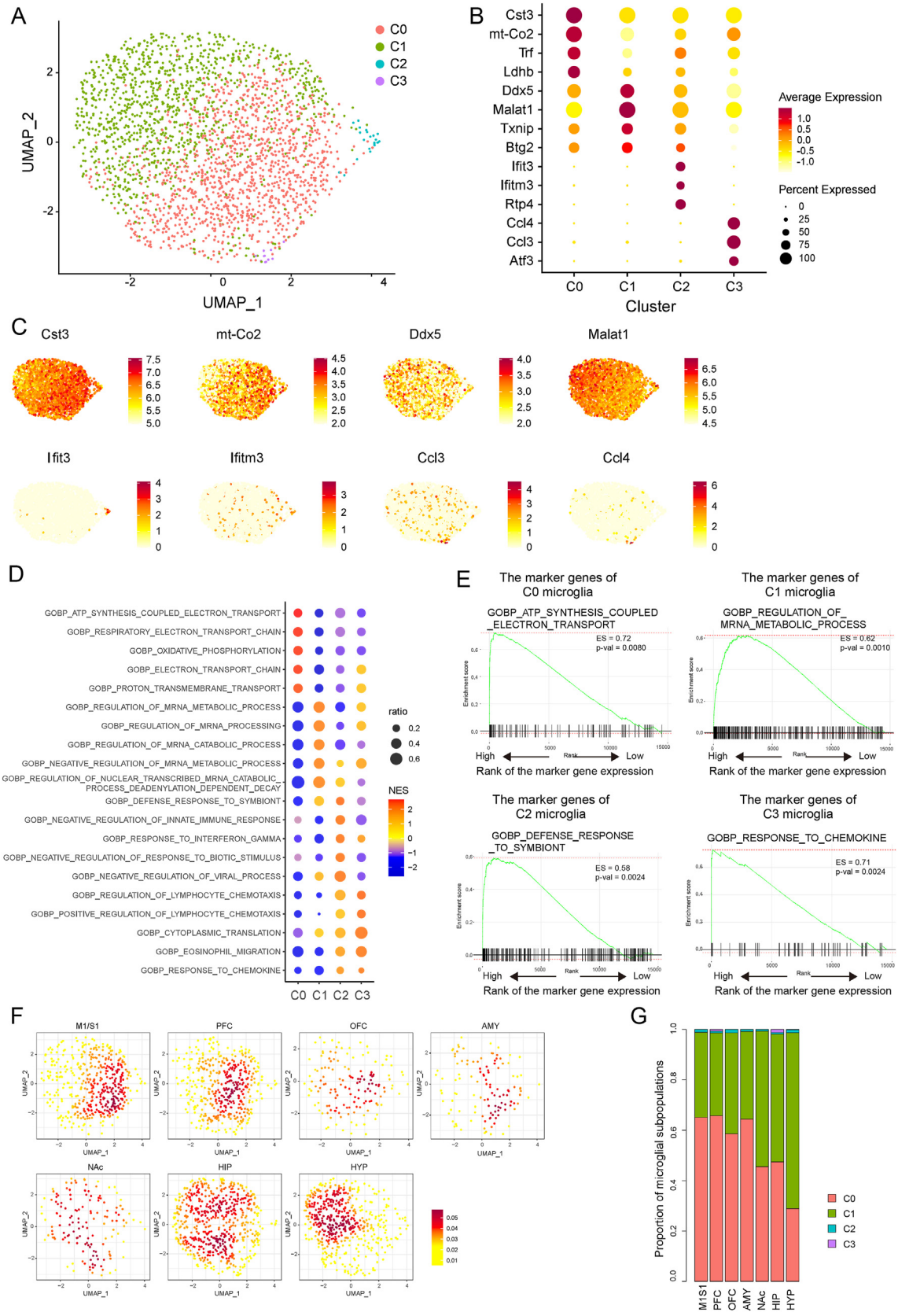

Fig. 2. Microglial subpopulations in the resting brain are differentially distributed across brain regions.
(A) UMAP plot showing the clusters of microglial subpopulations combined from multiple brain regions (C0 microglia, 1228 cells; C1 microglia, 1132 cells; C2 microglia, 22 cells; C3 microglia, 11 cells). (B) Bubble chart showing the marker genes of microglial subpopulations with the percentage of expressed genes (bubble size) and the averaged expression (color). (C) UMAP plot showing single-cell expression of the indicated marker genes. (D) Bubble chart showing the gene sets enriched in the marker genes of microglial subpopulations with the proportion of marker genes contributing to the gene set enrichment (bubble size) and the normalized enrichment score (NES) (color). (E) Enrichment plots

with Seurat 4[8] resulted in the transcriptome data of EGFP-expressing cells (2437 cells), N9 cells (302 cells), and HEK293-like cells (1004 cells) after removing low-quality cells and doublets (Fig. 1B). Cluster analysis with uniform manifold approximation and projection (UMAP) segregated EGFP-expressing cells, N9 cells, and HEK293-like cells, as expected (Fig. 1B and C). EGFP-expressing cells abundantly expressed microglia-associated genes, but those associated with central nervous system (CNS)-associated macrophages and neutrophils at negligible levels (Fig. 1D; see Supplementary Table 1 for the cell type-specific genes). Thus, most EGFP-expressing cells were microglia and designated as such. By contrast, N9 cells showed lower expression of microglia-associated genes and conventional microglia markers, Iba-1 and Cd11b. Furthermore, marker genes of single-cell clusters of microglia showed only a small overlap (50 genes) with those of N9 cells and no overlap with those of HEK293-like cells (Fig. 1E). In Gene Ontology (GO) enrichment analysis,[9] the marker genes of microglia enriched GO terms distinct from those of N9 cells and HEK293-like cells (Fig. 1F), suggesting an unexpected difference between microglia in the resting brain and microglia-like N9 cells.

Then we examined the transcriptome heterogeneity of microglia combined from multiple brain regions. Subclustering with UMAP revealed four microglial subpopulations annotated as C0, C1, C2, and C3 microglia with distinctive marker genes, after the clustering resolution was adjusted (Fig. 2A, B, and 2C). C0 and C1 microglia were two continuous subpopulations that covered most microglia in the resting brain in combination, whereas C2 and C3 microglia were minor subpopulations (Fig. 2A and B). We performed gene set enrichment analysis (GSEA)[10] for the genes with detectable expression ranked according to the enrichment in each subpopulation (Fig. 2D and E and Supplementary Table 2). C0 microglia enriched the expression of genes associated with mitochondrial respiration represented by GO terms such as “ATP synthesis coupled electron transport.” Highly ranked genes include those encoding Complexes I, III, IV, and V in electron transport chain, suggesting that C0 microglia have increased electron transport activity. C1 microglia enriched the expression of genes associated with mRNA processing represented by GO terms such as “regulation of mRNA metabolic process.” Highly ranked genes include those encoding spliceosome and RNA-binding proteins regulating RNA stability, suggesting that C1 microglia show altered mRNA slicing and degradation. C2 microglia enriched the expression of genes associated with interferon response represented by GO terms such as “Response to interferon gamma,” including signature genes of interferon response microglia (e.g., Ifit3, Ifitm3, Rtp4).[5] C3 microglia enriched the expression of genes associated with chemokine response represented by GO terms such as “Regulation of lymphocyte chemotaxis,” including signature genes of Ccl3/Ccl4-enriched microglia (e.g., Ccl3, Ccl4, Atf3).[5] The expression of genes associated with chemokine response were also enriched in C2 microglia as Ccl2 and Ccl12 were expressed in both C2 and C3 microglia. These findings show that the resting brain has distinct microglial subpopulations with different biological functions defined by separate signature genes. Microglia isolated from respective brain regions showed distinct transcriptome profiles, and the proportions of microglial subpopulations varied across brain regions (Fig. 2F and G). Microglia from the primary sensorimotor cortex (M1S1), prefrontal cortex (PFC), orbitofrontal cortex (OFC), and amygdala (AMY) enriched C0 microglia, and microglia from the hypothalamus (HYP) C1 microglia. Microglia from the nucleus accumbens (NAc) and hippocampus (HIP) contained C0 and C1 microglia of intermediate proportions. C2 microglia were distributed in all the brain regions. C3 microglia were only found in PFC and HIP, although the samples were too few to conclude their distribution. These findings suggest that the difference of microglial subpopulations contributes to brain region specificity of microglial transcriptome.

To seek microglial subpopulations activated by LPS and CSDS, we examined whether these stimuli would alter the expression of marker genes of respective microglial subpopulations. To isolate the effects of LPS on microglia from those on non-microglial cells, we generated primary microglia from female C57BL/6 N mice at 8–10 weeks old as previously described,[11] treated these cells with or without LPS at 100 ng/ml (purified from *E. coli* 055:B5, Sigma-Aldrich) for 4 h, purified total RNA with RNAdvance Cell (Beckman Coulter), and performed bulk RNA-seq analysis with SMART-Seq v4 (#634889, Takara Bio), Nextera XT (Illumina), and HiSeq X (Illumina). We converted the expression levels on Log2 scale to Z-scores within the variability of all detected genes. We used primary microglia because they expressed distinct microglial signature called ‘sensome’[12] such as Tlr2/4 for sensing endogenous ligands and microbes as highly as microglia isolated from the brain and more than N9 cells (Fig. 3A and B). LPS increased the expression of C2 marker genes (Fig. 3C). The expression of C3 marker genes also tended to be increased. In addition, we analyzed CSDS-induced expression changes of microglial subpopulation marker genes with previously published DNA microarray data (here PFC and NAc data combined) of male wild-type and TLR2/4 double knockout mice (TLR2/4-DKO) at 8–14 weeks old at the time of analysis.[6] CSDS increased the expression of C1 and C3 marker genes in wild-type microglia, and the expression of C1, but not C3, marker genes was increased in TLR2/4-DKO microglia (Fig. 3D). Thus, LPS and CSDS increased the expression of distinct (C2 marker genes for LPS and C1 marker genes for CSDS), but overlapping (C3 marker genes for both), signature genes of microglial subpopulations. The marker genes contributing to LPS- and CSDS-induced changes were also identified (Supplementary Table 3).

In this study, using scRNA-seq analyses, we identified four microglial subpopulations with distinct transcriptome signatures in the resting brain. These subpopulations include two novel subpopulations expressing the marker genes associated with electron transport activity (C0 microglia) and mRNA slicing and degradation (C1 microglia), respectively, besides previously reported minor subpopulations. The proportions of these microglial subpopulations varied across brain regions, especially between cerebral cortices (C0 dominant) and the hypothalamus (C1 dominant). Our findings suggest that LPS and CSDS stimulate distinct microglial subpopulations, C2 and C1 microglia, respectively. Consistently, the effect of CSDS on C1 marker genes was independent from TLR2/4. Notably, C2 marker genes upregulated by the TLR4 ligand LPS were unaffected by CSDS, which activates microglia via TLR2/4. Thus, the effects of TLR4 signaling depend on the conditions surrounding microglia. Since CSDS upregulates marker genes of C1 microglia enriched in the hypothalamus with high blood-brain barrier (BBB) permeability,[13] CSDS-induced BBB impairment could be involved in microglial activation.[14] The roles of the microglial subpopulations identified here in various conditions, including

showing the profile of the running enrichment score and the positions of gene set members on the rank-ordered list for the indicated GO terms and microglia subpopulations. (F) Density plots showing the UMAP-projected distribution of microglia isolated from respective brain regions (444 cells in the primary sensorimotor cortex (M1S1), 430 cells in the prefrontal cortex (PFC), 145 cells in the orbitofrontal cortex (OFC), 118 cells in the amygdala (AMY), 145 cells in the nucleus accumbens (NAc), 582 cells in the hippocampus (HIP), and 529 cells in the hypothalamus (HYP)). (G) Bar plots of the proportions of microglial subpopulations in respective brain regions. (For interpretation of the references to color in this figure legend, the reader is referred to the Web version of this article.)

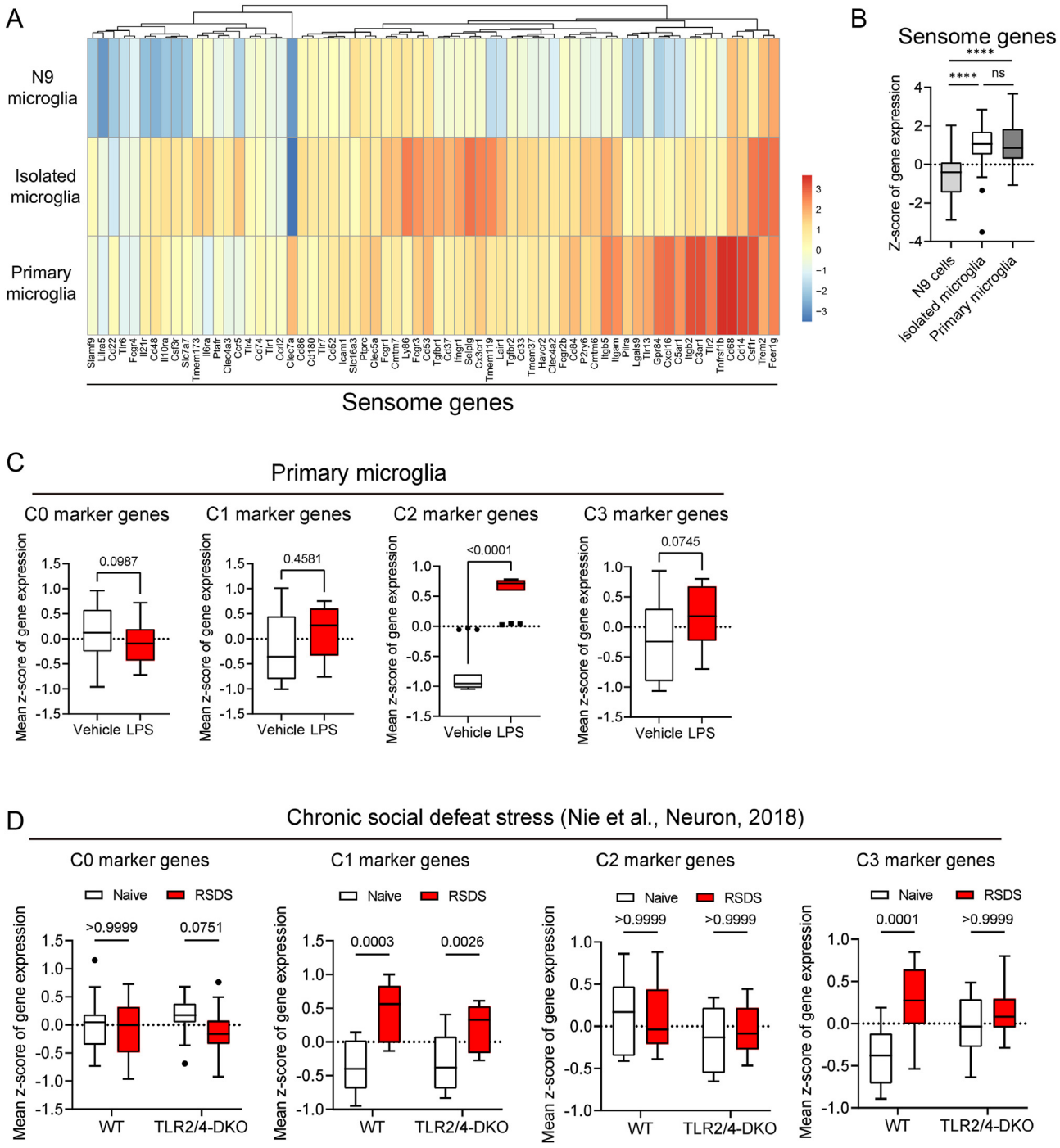

Fig. 3. LPS and CSDS increase the expression of marker genes of distinct microglial subpopulations.
(A, B) Heatmap (A) and box-whisker plot (B) showing Z-scores of gene expression of sensome genes (66 genes) in N9 cells, isolated microglia, and primary microglia. ****P < 0.0001 for Bonferroni's multiple comparisons test. (C, D) Box-whisker plots showing Z-scores of gene expression of the marker genes of microglial subpopulations in primary microglia with vehicle or LPS (averaged from 3 to 4 wells, respectively) (C) and in microglia isolated from PFC and NAc of wild-type (WT) and TLR2/4-DKO mice without or with CSDS (Naïve or CSDS, respectively) (averaged from 3 to 4 mice for each group) (D). The analyses include 35 genes for C0, 8 genes for C1, 15 genes for C2, and 26 genes for C3 in (C) and 27 genes for C0, 6 genes for C1, 11 genes for C2, and 23 genes for C3 in (D). The gene numbers in (D) are fewer than those in (C), because some genes detected by RNA-seq are not included in the DNA microarray data. P values shown in the graphs were calculated by paired *t*-test (C) and by Bonferroni's post hoc test following two-way ANOVA (D), respectively.

stress and neuroinflammation, and their mechanisms remain to be investigated.

Declaration of competing interest

The authors declare no conflict of interest.

Acknowledgments

We thank Dr. Shuh Narumiya for kindly providing CX3CR1-EGFP mice, Misako Takizawa for secretarial help, and Hiroko Iwamura for technical assistance. This study was supported in part by AMED, Japan grants (JP22gm0910012 and JP22wm0425001 to T.F.),

KAKENHI grants (18H05429 and 21H04812 to T.F., and 19K16372 to M.T.).

Appendix A. Supplementary data

Supplementary data to this article can be found online at https://doi.org/10.1016/j.jphs.2022.12.010.

References

1. Rivest S. Regulation of innate immune responses in the brain. *Nat Rev Immunol*. 2009;9(6):429–439.
2. Wake H, Moorhouse AJ, Jinno S, Kohsaka S, Nabekura J. Resting microglia directly monitor the functional state of synapses in vivo and determine the fate of ischemic terminals. *J Neurosci*. 2009;29(13):3974–3980.
3. Colonna M, Butovsky O. Microglia function in the central nervous system during health and neurodegeneration. *Annu Rev Immunol*. 2017;35:441–468.
4. Keren-Shaul H, Spinrad A, Weiner A, et al. A unique microglia type associated with restricting development of Alzheimer's disease. *Cell*. 2017;169(7):1276–1290.
5. Hammond TR, Dufort C, Dissing-Olesen L, et al. Single-cell RNA sequencing of microglia throughout the mouse lifespan and in the injured brain reveals complex cell-state changes. *Immunity*. 2019;50(1):253–271. e6. ;169(7):1276-1290.e17.
6. Nie X, Kitaoka S, Tanaka K, et al. The innate immune receptors TLR2/4 mediate repeated social defeat stress-induced social avoidance through prefrontal microglial activation. *Neuron*. 2018;99(3):464–479. e467.
7. Hirbec H, Marmai C, Duroux-Richard I, et al. The microglial reaction signature revealed by RNAseq from individual mice. *Glia*. 2018;66(5):971–986.
8. Hao Y, Hao S, Andersen-Nissen E, et al. Integrated analysis of multimodal single-cell data. *Cell*. 2021;184(13):3573–3587. e29.
9. Raudvere U, Kolberg L, Kuzmin I, et al. Profiler: a web server for functional enrichment analysis and conversions of gene lists (2019 update). *Nucleic Acids Res*. 2019;47(W1):W191–W198.
10. Mootha VK, Lindgen CM, Eriksson K, et al. PGC-1alpha-responsive genes involved in oxidative phosphorylation are coordinately downregulated in human diabetes. *Nat Genet*. 2003;34(3):267–273.
11. Sakate R, Nishiyama M, Fukuda Y, et al. The transcription factor Hhex regulates inflammation-related genes in microglia. *J Pharmacol Sci*. 2022;149(3):166–171.
12. Hickman SE, Kingrey ND, Ohsumi TK, et al. The microglial sensome revealed by direct RNA sequencing. *Nat Neurosci*. 2013;16(12):1896–1905.
13. Broadwell RD, Sofroniew MV. Serum proteins bypass the blood-brain fluid barriers for extracellular entry to the central nervous system. *Exp Neurol*. 1993;120(2):245–263.
14. Menard C, Pfau ML, Hodes GE, et al. Social stress induces neurovascular pathology promoting depression. *Nat Neurosci*. 2017;20(12):1752–1760.